# The performance of structured and unstructured grids on wind simulations around a high-rise building

IOP Conf. Series: Materials Science and Engineering **700** (2019) 012001 doi:10.1088/1757-899X/700/1/012001

# The performance of structured and unstructured grids on wind simulations around a high-rise building

**T-O Hågbo[1*], K E T Giljarhus[1], S Qu[2] and B H Hjertager[1]**

[1] University of Stavanger, Norway
[2] Harbin Engineering University, China

Corresponding author: trond-ola.hagbo@uis.no

**Abstract.** In this study, computational fluid dynamics has been applied to analyze the performance of both structured and unstructured meshes when used in steady-state simulations of wind in an urban area. This case specifically examines the wind environment around a single high-rise building with the geometry of 1: 1: 2 (length, width, height) within the atmospheric boundary layer.The Reynolds-averaged Navier-Stokes simulations were conducted using OpenFOAM, with grids generated with *blockMesh*, *snappyHexMesh*, and *Pointwise*. A set of coarse meshes and a set of fine meshes were used for comparison.Minor differences in the flow pattern were observed depending on the mesh type used, including the reattachment lengths, the drag coefficients, the velocity profiles, and the positioning of the vortex leeward of the high-rise building. However, the main flow features were the same, indicating that for simulations where overall flow features are of importance there is high flexibility in choice of meshing technique.

## 1. Introduction

In the recent decade, Computational fluid dynamics (CFD) has been increasingly applied to solve wind engineering problems, such as pedestrian wind discomfort and wind loads on buildings and bridges. In validation exercises of a single building, a structured mesh is often used. However, performing simulations on complex geometries, such as urban areas, requires complex meshes. Due to the indispensably high irregularity of these meshes, they can be time-consuming, complicated, and sometimes impossible, to create using a structured type of mesh. Alternatively, an unstructured mesh can be made. Their notable features include flexibility and adaptation capability[1].

As the usage of unstructured meshes is necessary for some applications, it is essential to know their performance in flow simulations and their associated accuracy. For some applications, a relatively coarse and unstructured mesh is sufficient and the most effective usage of computational power and time. There are cases where only the main flow structure is of interest, and when there is high uncertainty associated with other parameters of the simulation. For example, when simulating wind through an actual urban area to study pedestrian wind comfort.

In this study, CFD has been applied to analyze the performance of both structured and unstructured meshes when used in steady-state simulations of wind in an urban area. This case specifically examines the wind environment around a single high-rise building with the geometry

of 1: 1: 2 (length, width, height) within the atmospheric boundary layer (ABL). For the sake of detailed examinations, the flow past a simple shape, such as a high-rise building, seems to be more practical than in an actual urban environment.

Wind tunnel experiments on the high-rise building have been conducted by Meng and Hibi[2], with numerous other sources examining wind simulation studies of identical geometry. Examples include: Yoshie et al.[3], Tominaga et al.[4], Shao et al.[5], Gousseau et al.[6], Dadioti and Rees[7], and Liu and Niu[8]. The papers listed mostly focus on comparing various turbulence models and or transient simulations.

While unstructured meshes are necessary for some applications, the majority of existing research on the high-rise building benchmark case utilizing structured meshes. Therefore, this study will evaluate the performance of various mesh types, both structured and unstructed, in urban wind simulations to improve the understanding of the mesh type dependency.

The paper will evaluate mesh performance by first defining the computational domain. Second, the differences in grids used are illustrated by presenting coarse meshes. Then, the numerical setup is described in detail. In the last part of the methodology section, all the simulation cases are listed subsequently. The results are then presented and discussed, starting with the differences in reattachment lengths and drag coefficient, then moving towards other general flow features such as the flow structure and velocity profiles.

## 2. Methodology

This section describes the computational methodology. As the accuracy and reliability of CFD simulations can easily be compromised, best practice guidelines (BPG) have been developed for properly conducting CFD analysis of the wind environment in urban areas. These guidelines are based on cross-comparison between CFD simulations, wind tunnel experiments, as well as fields measurements on several cases. The BPG provided by Franke et al.[9] and Tominaga et al.[10] were carefully followed to set up the simulations.

### *2.1. Computational domain*

The computational domain size is identical for all the simulations conducted. The dimensions are $21.5b \times 13.75b \times 11.25b$ in the $x$ (length), $y$ (width) and $z$ (height) directions correspondingly and an overview is illustrated in Figure 1. $b$ is the width and length of the building which height is $2b$. In the experiments, $b$ was 0.08 m[2], and the same scale was used in the simulations.

Both the width and the height of the domain replicate the geometry of the wind tunnel setup, as recommended by the BPG. Also, the resulting blockage ratio is approximately 1.3 %, which is well within the suggested maximum value of 3 % recommended by the BPG, as proposed by Beatke et al.[11].

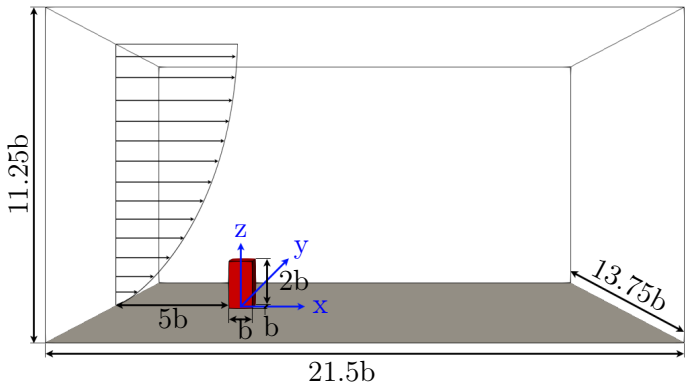


**Figure 1** Overview of the computational domain.

The length upstream of the building is $5b$, which is consistent with previous numerical studies such as [3, 4, 5, 7, 8]. Except for Tominaga et al.[4], all the other studies listed above were performed using a length downstream of the building of $21b$. Tominaga et al. used $21.5b$, which is used in this study.

### *2.2. Computational grids*

The main parameter reviwed in this study is the mesh type and its performance when used in wind simulations in urban areas. The grids used in this study were generated with either a built-in mesh generator in OpenFOAM, *blockMesh* or *snappyHexMesh*, or the commercial mesh generation software *Pointwise*[12]. The different meshing utilities are described below.

***blockMesh*** is suitable for highly simple geometries, such as the case at hand. It works by dividing the computational domain into multiple hexahedral blocks. These blocks can be stretched and bent to ensure proper cell density near walls and in specific areas where high flow gradients are emerging. All the meshes generated with *blockMesh* are structured.

***snappyHexMesh*** is a hex-dominant, unstructured mesh generator suitable for more complex geometries. It required an already existing base mesh, generated in this case by *blockMesh*, and an object file holding information of the triangulated surface geometries. *snappyHexMesh* snaps the mesh to the surface of the object file and iteratively refines the mesh close to the surfaces of choice.

***Pointwise*** is an advanced and highly flexible commercial mesh generation tool with the ability to create a variety of mesh types, both structured and unstructured, as well as hybrid types. For this study, *Pointwise* was used to generate both structured meshes entirely consisting of hexagons, and unstructured meshes constructed of prisms.

Figure 2 and Figure 3 illustrate the main differences in the mesh types used. Only examples of the coarse grids are illustrated.

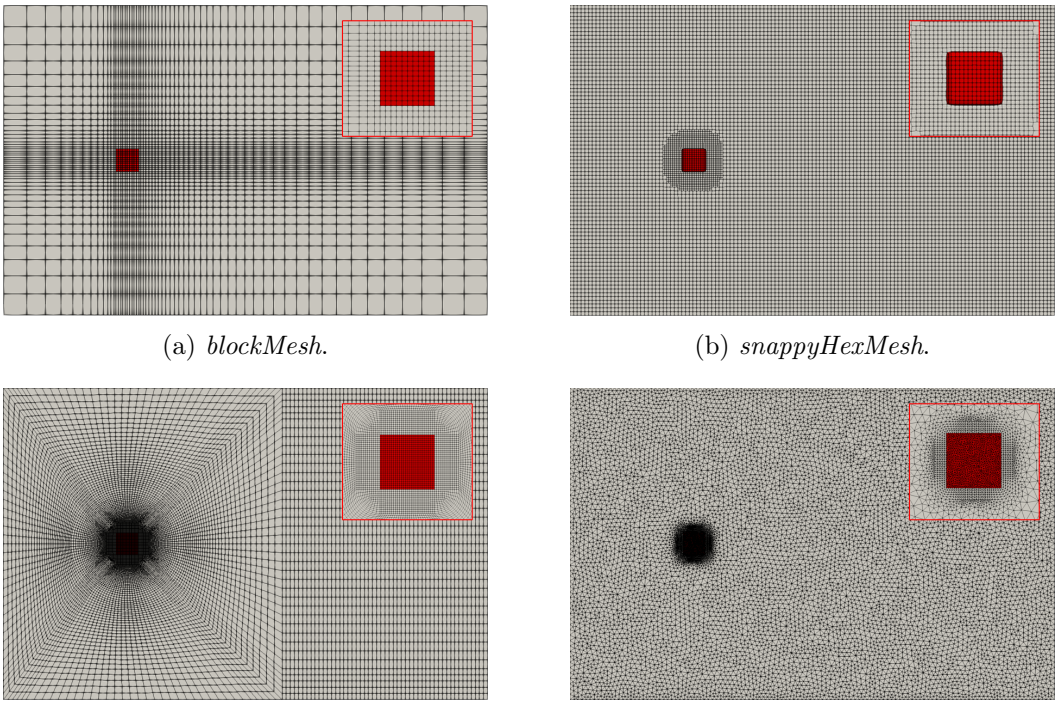

(a) *blockMesh.* (b) *snappyHexMesh.*

(c) *Pointwise, structured.* (d) *Pointwise, unstructured.*

**Figure 2.** Top view of the grid types showing the grid on the ground and the roof of the building. Inset shows a close-up near the building.

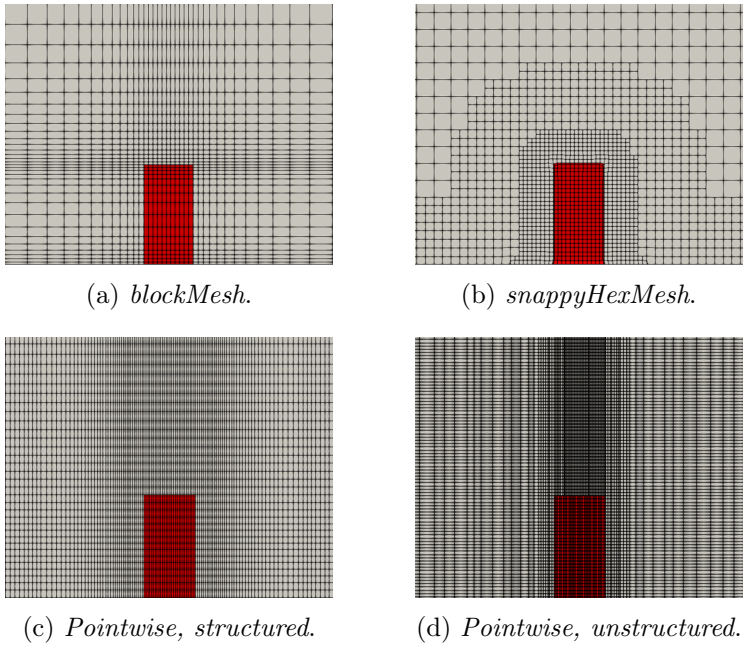

(a) *blockMesh*. (b) *snappyHexMesh*.

(c) *Pointwise, structured*. (d) *Pointwise, unstructured*.

**Figure 3.** Front view of the grid types at $x = 0$.

The configurations of the fine grid versions are similar, but with more cells and smaller cell widths for the cells in contact with the building or the ground. For the meshes generated with *blockMesh*, an even higher stretching has been applied. For the meshes generated with *snappyHexMesh*, proper cell width is obtained by adding more refinement levels near the building and ground. The computational cases with different meshes are summarized in Table 1. For some of the mesh types have a few different versions within the type been used in the simulations for comparison.

*2.3. Numerical setup and other parameters*

The turbulent wind flow pattern around the high-rise building was obtained by solving the incompressible, three-dimensional steady Reynolds-averaged Navier-Stokes (RANS) equations with the finite volume method. The Reynolds number based on $H$ (building height) and $U_H$ (inflow velocity at $z = H$) was $2.4 \times 10^4$. The pressure-velocity coupling was handled by the SIMPLE algorithm, and second-order discretization schemes were used for the convection terms of the governing equations. The convergence criteria for the scaled residuals were set to drop by four orders of magnitude for $U$, $k$, and $\epsilon$ and three orders of magnitude for $p$. The simulations were conducted using the OpenFOAM toolbox, which is an open-source CFD software package.

The vertical distributions of the quantities at the inflow boundary were set on the basis of the wind tunnel experiment[2] to assure similar conditions. As the vertical profile of the streamwise velocity approximately obeyed a power law, the velocity at the inlet was set to be $U = U_H(z/z_H)^{0.27}$, where $U_H$ is the wind speed at reference height $z_H$. $z_H$ was set to be the height of the building, $2b = 0.16\,\mathrm{m}$, with an $U_H$ of $4.5\,\mathrm{m\,s^{-1}}$ following the measurements. The profiles of both the turbulent kinetic energy, $k$, and the dissipation rate, $\epsilon$, were interpolated from the experimental data.

The outlet of the domain was set to zero static pressure with zero gradient for the remaining variables. For the lateral and top boundaries, the slip condition was used for all the variables. No-slip conditions were applied to the building and the ground. The roughness length $z_0$ on the ground was set to $1.8 \times 10^{-4}$, in accordance with Yoshie et al.[3].

Two near-wall treatment methods were used. For the simulation cases using the fine meshes ("the fine simulations"), no wall functions were applied. Wall functions were implemented for the cases using a coarse mesh ("the coarse simulations"). A logarithmic law for smooth walls was used on the building, and a logarithmic law, including a roughness parameter was applied for the ground.

Turbulent closure was provided by three different turbulence models for incompressible flows. For the "coarse simulation", both the standard $k$-$\epsilon$ model (SKE)[13] and the realizable $k$-$\epsilon$ model (RKE)[14] were used. The RKE was chosen as a reference since it is recommended by Blocken et al.[15] in the application of pedestrian wind environment simulations. In the "fine simulations", the cells close to the walls are presumably mostly within the viscous sublayer, and a low-Reynolds number model is more appropriate. The Lien and Leschziner low-Reynolds number $k$-$\epsilon$ model (LLKE)[16] was chosen.

*2.4. Simulation cases*

The setup for all the simulations was identical except for three changes:

- Grid type – coarse/fine, structured/unstructured, and generated with different meshing utility.
- Wall functions - the coarse simulations used wall functions as opposed to the fine simulations that did not.
- Turbulence models - the coarse simulations used either the SKE or the RKE while the fine simulations used the LLKE.

In Table 1, the "Case name" column the "C" stands for coarse mesh while the "F" indicates that a fine mesh has been used. The first two letters in the "Mesh" column represents the meshing utility used for creating the final mesh, with "BM" standing for *blockMesh*, "SH" for *snappyHexMesh* and "PW" for *Pointwise*.

**Table 1.** List of simulation cases.

| Case name | Mesh | Cells | Turbulence model | $y^+$ (average) building | ground |
|---|---|---|---|---|---|
| C1 | BMC1 | 104 k | SKE | 152 | 99.3 |
| C2 | — " — | — " — | RKE | 152 | 98.5 |
| C3 | BMC2 | — " — | SKE | 29.5 | 38.0 |
| C4 | — " — | — " — | RKE | 29.1 | 37.5 |
| C5 | SHC1 | 191 k | SKE | 30.0 | 117 |
| C6 | — " — | — " — | RKE | 29.7 | 117 |
| C7 | SHC2 | 519 k | SKE | 29.9 | 58.7 |
| C8 | — " — | — " — | RKE | 29.6 | 58.5 |
| C9 | PWC1 | 674 k | SKE | 117 | 61.5 |
| C10 | — " — | — " — | RKE | 114 | 61.4 |
| C11 | PWC2 | 3.66 M | SKE | 13.7 | 50.1 |
| C12 | — " — | — " — | RKE | 13.8 | 56.9 |
| F1 | BMF1 | 20.6 M | LLKE | 7.43 | 2.83 |
| F2 | SHF1 | 16.7 M | —— " —— | 2.93 | 4.10 |
| F3 | SHF2 | 27.2 M | —— " —— | 2.14 | 2.62 |
| F4 | PWF1 | 3.59 M | —— " —— | 3.65 | 0.97 |
| F5 | PWF2 | 8.68 M | —— " —— | 2.22 | 1.20 |

The mesh BMC1 has no stretching of the cells whatsoever, but BMC2 has, which is the mesh presented in Figure 2a and Figure 3a. SHC2/SHF2 has one more refinement level to the ground compared to SHC1/SHF1, which is presented in Figure 2b and Figure 3b. PWC1/PWF1 are structured meshes, while PWC2/PWF2 are unstructured. PWC2 is here categorized as coarse, even though the number of cells is high. It was decided to include C11 and C12, although the average $y^+$ values at the building are far lower than recommended for the turbulent models used.

## 3. Results and Conclusion

### *3.1. Reattachment lengths and drag coefficients*

Table 2 gives the reattachment lengths and the drag coefficients for all the simulated cases, a few results from the literature, and the experimental data. $X_R$ is the distance from the roof edge facing the wind where flow separation occurs to the point where the flow reattaches to the roof. $X_F$ is the length leeward of the building where the flow reattaches to the ground.

Flow reattachment on the roof was obtained for four cases: C11, C12, F3, and F5. For the coarse simulations, it was achieved only when a mesh consisting of far more cells than the other coarse meshes was used. The two cases that obtained flow reattachment on the roof for the fine meshes were also the two cases with the lowest average $y^+$ values at the building. In general, a large number of grid cells are needed to fully resolve the roof vortex, which is not achieved for the coarse meshes. $X_F$ was 9 to 12 % longer for all the coarse simulations when using the turbulence model RKE instead of SKE. When using SKE $X_F$ was in the range $2.74b$ to $2.87b$ when excluding C11. The range for RKE was $2.99b$ to $3.12b$, excluding C12. For LLKE and the fine simulations, the range was considerably larger, $2.23b$ to $3.42b$.

The drag coefficients, $C_D$, for the coarse simulations are somewhat lower than for the fine simulations, 0.809 to 1.076 compared to 1.071 to 1.347. When excluding the results from F5, the variance within the fine simulations is much less compared to the coarse simulations. This is expected since these meshes are closer to mesh-independent results.

**Table 2.** Reattachmenth lengths and drag coefficients.

| Case | $X_F/b$ | $X_R/b$ | $C_D$ | Case | $X_F/b$ | $X_R/b$ | $C_D$ |
|---|---|---|---|---|---|---|---|
| C1 | 2.84 | - | 0.994 | F1 | 3.42 | - | 1.071 |
| C2 | 3.12 | - | 0.855 | F2 | 2.65 | - | 1.081 |
| C3 | 2.74 | - | 1.030 | F3 | 2.53 | 0.16 | 1.113 |
| C4 | 2.99 | - | 0.948 | F4 | 2.83 | - | 1.118 |
| C5 | 2.80 | - | 0.880 | F5 | 2.23 | 0.21 | 1.347 |
| C6 | 3.11 | - | 0.811 | | | | |
| C7 | 2.80 | - | 0.881 | C SKE[4] | 2.7 | - | N/A |
| C8 | 3.14 | - | 0.809 | C SKE[5] | 2.4 | - | N/A |
| C9 | 2.87 | - | 1.076 | C SKE[7] | 2.68 | 0.50 | N/A |
| C10 | 3.21 | - | 1.002 | C RKE[7] | 5.37 | 0.50 | N/A |
| C11 | 2.61 | 0.42 | 1.061 | F SKE[8] | 3.50 | 0.58 | N/A |
| C12 | 2.85 | 0.41 | 0.972 | Exp.[2] | 1.42 | 0.52 | N/A |

*3.2. Flow pattern and velocity distribution*

Figure 4 shows the flow pattern in a vertical slice through the centre of the building, viewed from the side. All simulations show similar flow features, with a stagnation point in front of the building at approximately 3/4 of the building height, and a large recirculation zone behind the building.

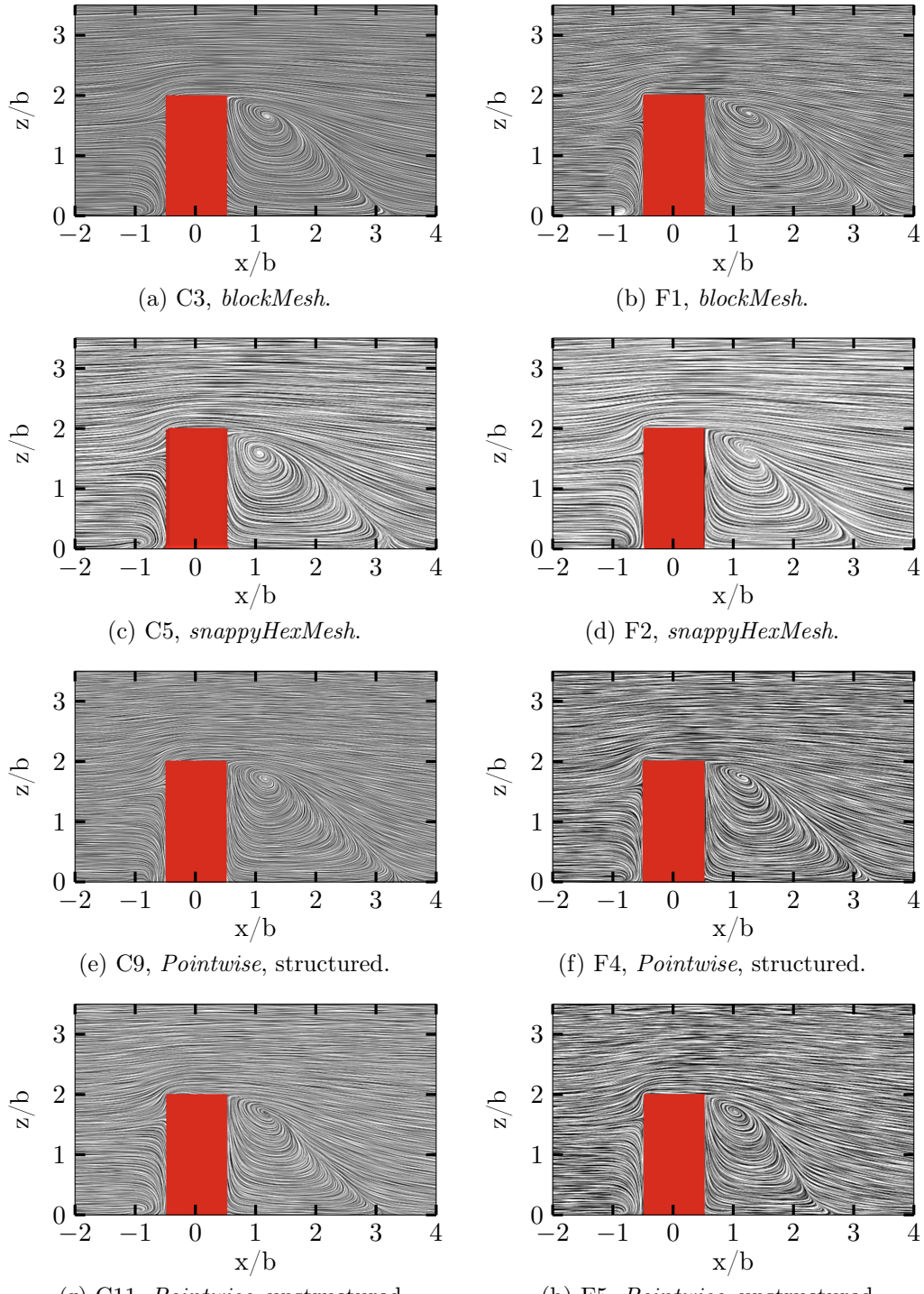


(a) C3, *blockMesh*. (b) F1, *blockMesh*.

(c) C5, *snappyHexMesh*. (d) F2, *snappyHexMesh*.

(e) C9, *Pointwise*, structured. (f) F4, *Pointwise*, structured.

(g) C11, *Pointwise*, unstructured. (h) F5, *Pointwise*, unstructured.

**Figure 4**. Flow patterns using line integral convolution, side view at $y/b = 0$.

Figure 5 shows the horizontal distributions of the mean wind speed near the ground surface at $z/b = 0.125$. Only contour plots of two simulations were included, in addition to numerical and experimental results from the literature for reference. The other simulations gave similar results. Notice that the shape and placement of the contour lines are comparable between these simulations and the references. However, the wind velocity close to the ground is somewhat lower for all the simulations compared to the experiments and the C SKE case[5].

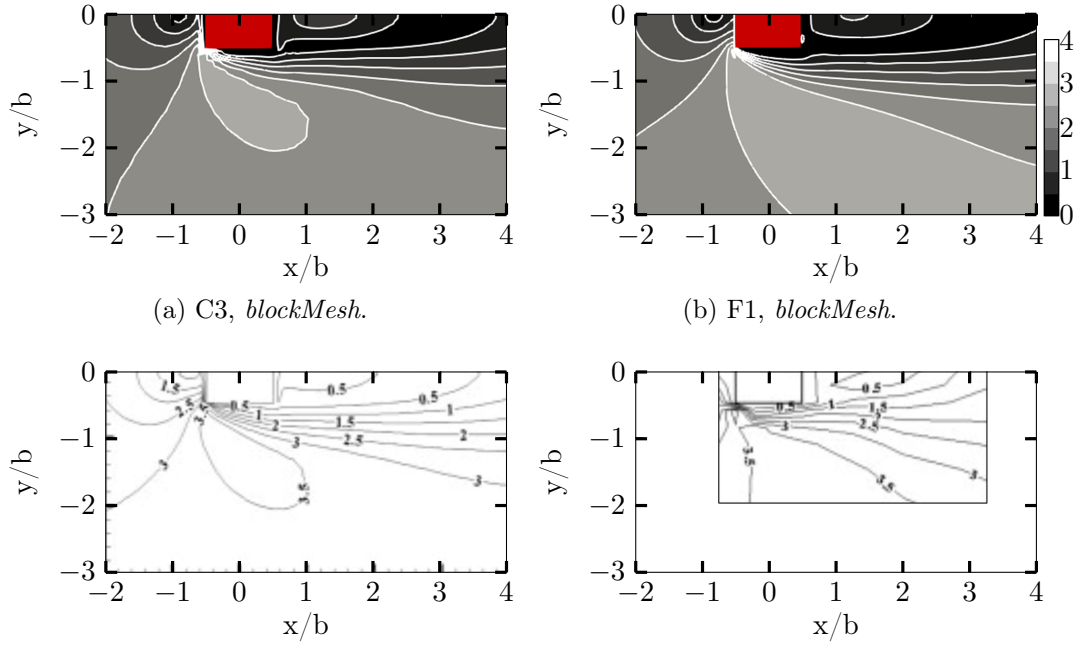


(a) C3, *blockMesh*. (b) F1, *blockMesh*.

(c) C SKE[5]. (d) Experimental data[2].

**Figure 5.** Velocity contour lines in m $s^{-1}$, top view at $z/b = 0.125$.

Figure 6 is a collection of vertical profiles of wind velocity in the x-direction placed on top of the measurement regions (indicated with dotted black lines). The crosses represent the experimental values, while the colored lines represent data sampled from the simulations. The simulation cases included are the same as in Figure 4. Lines and crosses on the left side of its sampling line represent negative values, hence that the wind is moving in the negative x-direction.

By comparing Figure 6a and Figure 6b, it is clear that the velocity profiles in the fine simulations vary less in the region leeward of the building roof compared to the coarse simulations. It indicates that the coarse grids have too few cells to have reached a resolution-independent result. The differences are evident in the region in particular, as high flow gradients are emerging, which need more cells to resolve the flow behavior.

When comparing the profiles to the experimental values, one cannot conclude that one mesh type is superior to the others. However, C5, F2, and F5 appear to produce velocity profiles the closest to the experimental values. Both C5 and F2 have unstructured meshes generated with *snappyHexMesh*, and F5 uses an unstructured mesh made with *Pointwise*.

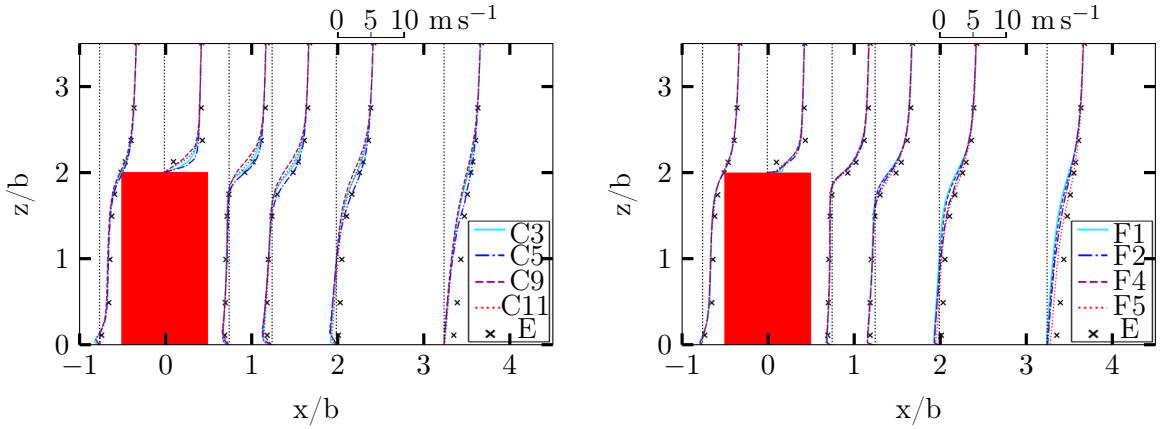


(a) Coarse simulations. (b) Fine simulations.

**Figure 6.** Vertical velocity profile comparison, side view at $y/b = 0$.

*3.3. Concluding remarks*

This study compared the use of different meshing techniques for simulating wind flow around a rectangular, high-rise building.

All flow simulations gave similar flow patterns, indicating that for simulations where overall flow features are of importance there is high flexibility in choice of meshing technique. The difference between the use of wall functions and wall-resolved simulations were also minor. Hence, it appears that a coarse and unstructured type of mesh can be sufficient in the applications where only the general flow features are of interest. This is the most flexible gridding technique for complex urban areas.

The reattachment lengths behind the building were considerably longer than in the experiments for all the simulations. This is in agreement with other RANS simulations in the literature. In general, the reattachment length is a highly sensitive parameter due to the transient nature of the flow. More advanced simulations using, for example, large eddy simulations, have been able to accurately predict the reattachment length, but even for such simulations there is high variability in the reported results [4, 6, 8].

**Acknowledgments**

This research is part of the Future Energy Hub Project funded by The Norwegian Research Council (project no.: 280458), The University of Stavanger, and local industry partners. We thank the anonymous reviewers for insightful and much-appreciated feedback.

## References

[1] Kim S E and Boysan F 1999 *J Wind Eng Ind Aerodyn* **81** 145–158
[2] Meng Y and Hibi K 1998 *J Wind Eng* **1998** 55–64
[3] Yoshie R, Mochida A, Tominaga Y, Kataoka H, Harimoto K, Nozu T and Shirasawa T 2007 *J Wind Eng Ind Aerodyn* **95** 1551–1578
[4] Tominaga Y, Mochida A, Murakami S and Sawaki S 2008 *J. Wind Eng Ind Aerodyn.* **96** 389–411
[5] Shao J, Liu J and Zhao J 2012 *J Built Environ* **57** 145–155
[6] Gousseau P, Blocken B and Van Heijst G 2013 *J Comp Fluids* **79** 120–133
[7] Dadioti R and Rees S J 2015 Validation of open source CFD applied to building external flows *Proc. BS2015, 14th Conf. Int. Build. Perform. Simul. Assoc.*
[8] Liu J and Niu J 2016 *J Built Environ* **96** 91–106
[9] Frank J, Hellsten A, Schlünzen H and Carissimo B 2007 *Quality Assurance and Improvement of Meteorological Models. University of Hamburg, Meteorological Institute, Center of Marine and Atmospheric Sciences*
[10] Tominaga Y, Mochida A, Yoshie R, Kataoka H, Nozu T, Yoshikawa M and Shirasawa T 2008 *J Wind Eng Ind Aerodyn* **96** 1749–1761
[11] Baetke F, Werner H and Wengle H 1990 *J Wind Eng Ind Aerodyn* **35** 129–147
[12] Pointwise The choice for CFD meshing `https://www.pointwise.com`
[13] El Tahry S 1983 *J Energy* **7** 345–353
[14] Shih T H, Liou W W, Shabbir A, Yang Z and Zhu J 1995 *J Comp Fluids* **24** 227–238
[15] Blocken B, Roels S and Carmeliet J 2004 *J Wind Eng Ind Aerodyn* **92** 849–873
[16] Lien F S and Leschziner M 1993 *J Fluids Eng* **115** 717–725